UDC 621.313 https://doi.org/10.20998/2074-272X.2023.1.01

S. Arslan, H. Mellah

Analysis and testing of internal combustion engine driven linear alternator

Introduction. *Internal combustion engine technology has been considered for the alternator system in the last two decades. Especially when considering fuel diversity, reliability, portability, power density, research studies are increasing day by day. In this respect, interest has been focused on linear generator studies.* ***Purpose***. *The goal of the research is to investigate the performance of a linear generator and its application to generate electrical energy from an internal combustion engine to solve the range problem of small electric powered vehicles. The generator, unlike a traditional generator, consists of a linear generator with a crank mechanism driven by an internal combustion engine.* ***Originality.*** *The configuration of the linear generator with internal combustion engine crank has not previously been reported.* ***Methods***. *The numerical solution of the generator was carried out by the finite element method in the Ansys Maxwell software in a cylindrical coordinate system. The effect of stroke length and frequency on voltage and output power was investigated by monitoring an external electrical load. A prototype linear generator has been designed and produced considering the sizing dimensions. The configuration can be used in power-hungry applications and increase the range of small electric vehicles.* ***Results***. *The results from simulation and practice are largely in agreement.* ***Practical value***. *A practical mechanical system was built comprising a linear generator connected to a 2.2 kW internal combustion engine via a crank connecting rod for analysis.* References 35, table 1, figures 15.

Key words: **linear generator, electric vehicle, hybrid vehicle, internal combustion engine.**

Вступ. *Останні два десятиліття розглядалася техніка двигуна внутрішнього згоряння для системи генератора змінного струму. Особливо з урахуванням різноманітності видів палива, надійності, портативності, питомої потужності кількість досліджень зростає з кожним днем. У зв'язку з цим інтерес був зосереджений на дослідженнях лінійних генераторів.* ***Мета***. *Метою дослідження є аналіз продуктивності лінійного генератора та його застосування для вироблення електроенергії від двигуна внутрішнього згоряння для вирішення проблеми запасу ходу малих електромобілів. Генератор, на відміну від традиційного, складається з лінійного генератора з кривошипно-шатунним механізмом, що рухається двигуном внутрішнього згоряння.* ***Оригінальність***. *Про конфігурацію лінійного генератора з кривошипом двигуна внутрішнього згоряння раніше не повідомлялося.* ***Методи***. *Чисельне рішення генератора проводилося методом скінченних елементів у програмі Ansys Maxwell в циліндричної системі координат. Вплив довжини та частоти ходу на напругу та вихідну потужність досліджували шляхом моніторингу зовнішнього електричного навантаження. З урахуванням габаритних розмірів розроблено та виготовлено прототип лінійного генератора. Конфігурація може використовуватися в енергоємних застосуваннях і збільшувати запас ходу невеликих електромобілів.* ***Результати***. *Результати моделювання та з практики переважно збігаються.* ***Практична цінність***. *Для аналізу було побудовано практичну механічну систему, що складається з лінійного генератора, з'єднаного з двигуном внутрішнього згоряння потужністю 2,2 кВт через шатун кривошипу.* Бібл. 35, табл. 1, рис. 15.

Ключові слова: **лінійний генератор, електромобіль, гібридний автомобіль, двигун внутрішнього згоряння.**

Introduction. Energy has become important for the developing world. Electrical energy has typically been produced using fossil fuels despite the harmful effects to the environment. Vehicles, and the internal combustion engine (ICE), are one of the major users of fossil fuel. Although electric vehicles have zero emissions, they suffer from a range and charging problems. However, with advances in battery and charging technology, the number of electric and electric/hybrid vehicles is increasing. Hybrid vehicles offer an alternative compared to traditional fossil fuel-based vehicles in the short and medium term. In addition, future technology, such as fuel cells, promises to solve the range problem in hybrid vehicles and is emission free. Further advances in battery technology (long life, fast charge-late discharge, high per unit mass capacity, and low cost) will reduce the disadvantages of electric/hybrid vehicles.

Further energy-generating technology can be incorporated in electric vehicles to improve the range and make use of electric or hybrid electric vehicles more attractive. It can be given as regenerative braking, regenerative suspension systems, solar panels, wind generator, thermo-electric generator, respectively.

In hybrid electric vehicles, the role of the ICE can be categorized into series, series-parallel, and parallel classes, according to its purpose in relation to the electrical propulsion. Various forms of ICE have been used in hybrid electric vehicles including two-stroke and four-stroke. The two-stroke engine offers higher power and speed, and lower vibration compared to the four-stroke engine [1]. Vibration is a major problem, especially at high speeds, and studies on the effects of vibration have been conducted between 10 Hz and 30 Hz [2-4]. The stroke length of the linear motion of the ICE equals the length of motion of the ICE piston. For example, in [5] the effective stroke length is 62 mm. In studies [2, 6-10], it has been shown that the free piston mechanism and the crank connecting mechanism exhibit a very similar movement profile. Newer forms of ICE, including the free piston system [11-13], are being investigated as multi-fuel, high efficiency, low emission options.

In the ICE, the linear force of the piston rod is turned into torque and rotational motion through the action of the crank rods and crankshaft. This rotational drive can be applied directly to the shaft a conventional rotating electrical generator. However, the linear motion of the piston rod can be used directly as a free piston mechanism for a linear motion drive [14, 15].

The moving part of a linear generator is arranged so that it moves back and forth freely. In order for a free-piston linear generator to operate with an ICE, the piston has first to be moved to compress the air-fuel mixture. This is difficult on the first stroke. Despite the limited number of studies on the initial state of the linear generator, some methods have been offered as solutions to the starting problem [16-25], including mechanical resonance [16-18], injection time control [23-26] or special control system [19-26].

Some studies [27, 28] have investigated the Wankel REX [29] and Otto REX [29], as these generate rotational drive directly that can be connected to a conventional electrical generator.

The goal of the paper is to investigate the generation of electrical energy numerically and experimentally by operating the tube type linear generator on an ICE with a crank connecting rod mechanism.

Investigation of linear generator with finite element analysis (FEA). A linear machine converts mechanical energy into electrical energy or converts electrical energy into mechanical energy via linear motion [11]. Designs may vary according to application, with different values of speed, frequency, stroke distance, and force. Different types of linear generator are detailed in [26, 27, 30]. The structure and working principle (induction, synchronous, transverse flux, or longitudinal flux) will determine the parameters for the electric generator. This study investigates the permanent magnet linear generator with longitudinal flux. The stroke length of the generator has been limited to allow use as tubular geometry and be coupled to an ICE. The tube-type geometry has advantages compared to the flat-type linear generators; it minimizes asymmetric forces between the moving magnet and primary windings, and has higher power-to-weight ratio, higher efficiency, and power density. However, having the magnet as the moving part, a deceleration force will occur between the primary windings and the moving magnet. As the flux density of the magnet increases, the generator output voltage and cogging force increase [31]. This force can be reduced by methods such as the geometry of the magnet, pole pitch ratio, split ratio and including slot pitch. This study has taken the design of the tubular generator as 4 magnetic poles and 6 primary windings, as shown in Fig. 1, for analysis.

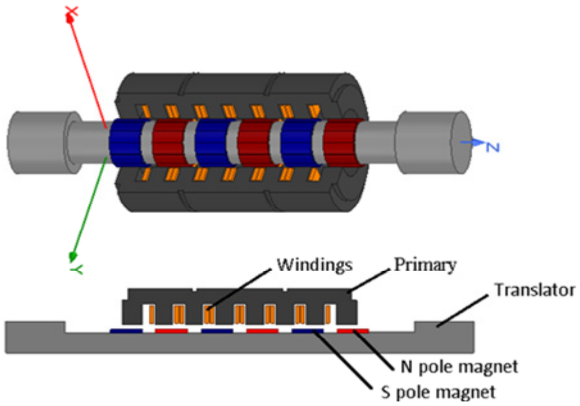

Fig. 1. 3-D and 2-D views of tube-shaped linear generator

Output parameters of circular linear machines can be calculated by using numerical analysis programs such as Ansys Maxwell 2D/3D, MotorSolve [32], Speed, etc.

Generator numerical analysis. The 3-D geometry of the linear generator can be converted to 2-D geometry for analysis by the finite element method, as this reduces computation time. 2-D FEA is often used to help in the design of electric machines, and determine parameters such as current density, magnetic flux distribution, winding inductance changes and electromagnetic force. The design parameters for the linear generator of this study are given in Table 1.

Table 1

Linear generator design parameters

Parameters	Value	Unit
Frequency	50	Hz
Airgap length	1	mm
Primary inner diameter	51	mm
Magnet width	20	mm
Alpha (pole pitch ratio)	0.72	
Beta (slot pitch ratio)	0.5	
Slot / Pole	6/4	
Slot filling factor	0.7	

2-D analysis of the linear generator. Values have been set for the moving force (magneto-static solution and transient solution), and winding inductance (magneto-static solution) for the simulation. In addition, two-dimensional numerical analyzes can be applied to analyze different situations (magnet shift technique [33], different magnet geometries [34], etc.) for reducing cogging force in the machine. The duration of the simulation and time steps were also set. The force on the moving part of the generator (in the seconder), magnetic flux density, magnetic field intensity, flux paths, and current density were determined in the simulation at each time step.

The simulation includes transient state and continuous state analysis of the 2-D plane selected to determine surface conditions. Mesh selection is very important, with a high resolution mesh applied in critical areas. For example, in time-dependent analysis, dense mesh resolution is used in areas of movement to increase the accuracy of the calculation of force.

Increasing working current will increase the current density in the conductive regions. The increase in power will increase losses and heat, which will require the thermal value of the generator to be increased and may require additional cooling.

The effect of variables such as a pole pitch ratio, inner diameter outer diameter ratio, and slot pitch ratio on parameters including cogging force, induced voltage, and losses, can be determined by parametric analysis. Figure 2 shows the electrical equivalent of the linear generator with and without load that is used for the numerical and experimental studies.

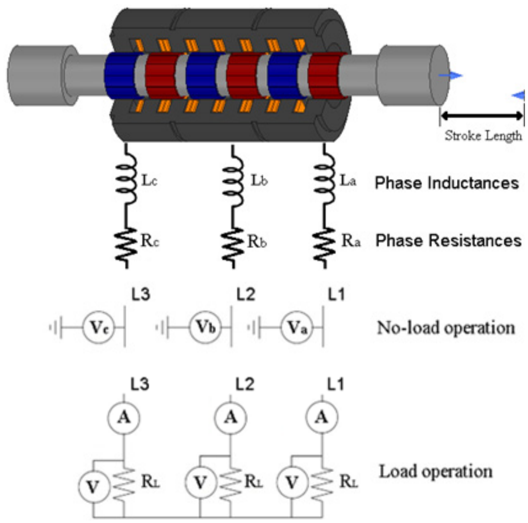

Fig. 2. Wiring diagram of linear generator for no-load and load condition

The phase windings have been configured with no-load in FEA transient state analysis to analyse the no-load condition and investigate the effect of frequency and stroke length on induced voltage.

Figure 3 shows how the induced voltage increases as the stroke length increases at constant frequency. Figure 3 also shows how the induced voltage increases as the frequency increases at constant stroke length. In fixed frequency operation, as the stroke length increases, the induced voltage increases, while in the loaded condition, the iron loss and copper loss increase and the induced voltage decreases at larger stroke lengths. The windings include inductance and so a capacitor of 100 μF has been connected in series with the phase windings and load in order to compensate for the effects [35]. Figure 2 shows the generator with a load connected to investigate the power generated; two load resistances were considered, 10 Ω and 30 Ω.

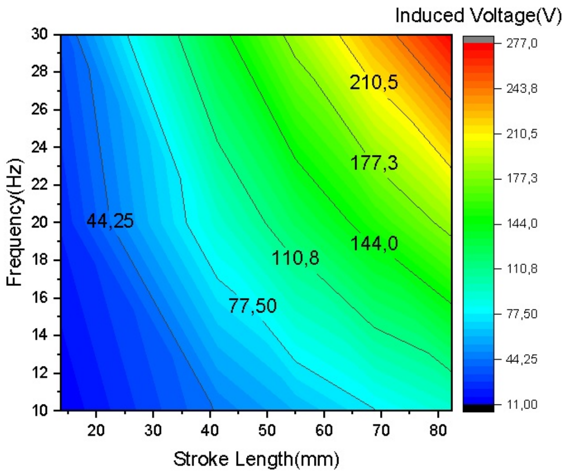

Fig. 3. Induced voltage according to stroke length and frequency in no-load condition.

The output power of the linear generator was investigated for stroke length and frequency for the two loads, with and without series capacitor (Fig. 4,*a*-*d*).

Figure 4 shows that output power increases with stroke length and frequency, and an optimum operating point can be determined. Figure 4 also shows that compensating for the winding reactance increases significantly the power delivered to the load at high frequencies. However, there is no increase in output power at low speeds. It would be important to determine the optimum value for the capacitor for the specific operating condition. This could include use of different capacitors for power compensation at different operating speeds of the generator.

In 2-D analysis, the effect of load resistance changes on the power and efficiency produced in the linear generator can be examined. Thus, maximum power and maximum efficiency are obtained according to the changing external load resistance. The variation of power generation and efficiency performance with different external load values is shown in Fig. 5.

According to the results, the efficiency is 83.7 % at 10 Ω, where the maximum power is obtained. However, one can note that as the external load increases, the efficiency increases significantly and the power decreases. The load value at which the efficiency is maximum (93.87 %) is 70 Ω. At the optimum load value (16 Ω), the power obtained from the generator is 787 W, the efficiency is 88 %.

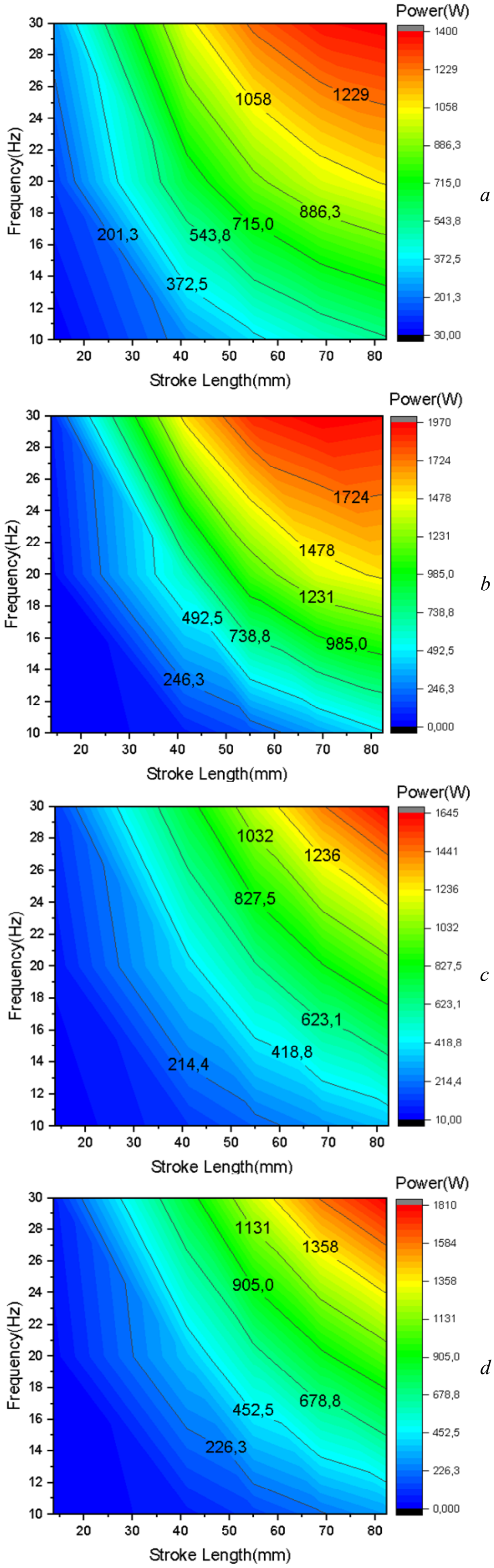

Fig. 4. Output power for stroke length and frequency: 10 Ω (*a*); 10 Ω with 100 μF capacitor (*b*); 30 Ω (*c*); 30 Ω with 100 μF capacitor (*d*)

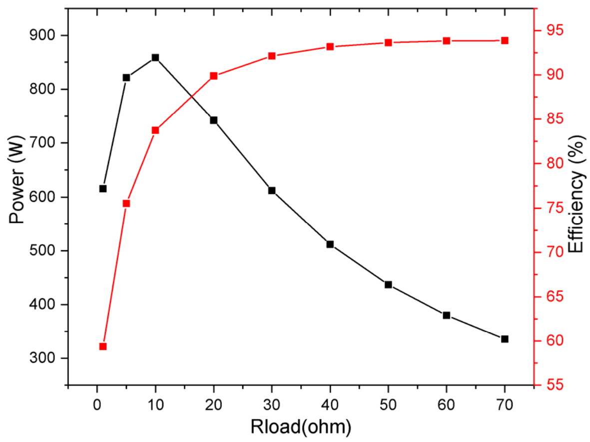

Fig. 5. Power and efficiency variation of the linear generator vs load resistance

Linear generator manufacture and testing. The linear generator in this study has been made in a tubular topology using the dimensions determined from the FEA. The primary laminates are produced from 0.5 mm M43 quality steel using laser cutting. 1020 quality steel is used for the moving secondary shaft, on which the magnets are mounted. The windings are wrapped on a mould made of delrin material. Figure 6 shows the individual components of the linear generator.

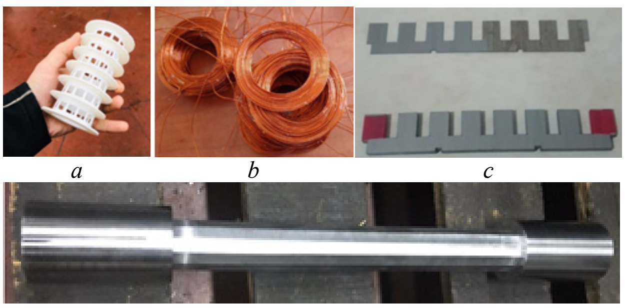

d

Fig. 6. Materials: CNC-produced winding mould (*a*); windings (*b*); laser-cut primary laminate (*c*); CNC-produced magnetless shaft (*d*)

Generator drive system. In a free piston system, the linear velocity is close to sinusoidal in form. For this study, an eccentric system with a crank mechanism has been designed to connect to an existing ICE to provide a sinusoidal linear speed profile. The Por-MAX CS-5200 2.2 kW gasoline engine (Fig. 7) has been used as ICE to provide the drive to the linear generator.

Fig. 7. ICE 2.2 kW

The ICE provides a power of 2.2 kW at 4000 rpm, giving a torque as given as (1), giving engine torque as 5.25 N·m. This value is calculated as the torque produced by the ICE:

$$T_m = 9550 \cdot P_m / N_m . \quad (1)$$

There was concern that the ICE could cause significant vibration and result in damage to the engine when connected to the linear generator and operated at low speeds. A reducer was therefore used to reduce these effects. The torque at the output of a reducer is proportional to its gear ratio, whereas the output speed of the reducer is inversely proportional to the gear ratio of the input speed, as in (2):

$$T_{rg} / T_{rc} = z_1 / z_2 . \quad (2)$$

The gear ratio of the reducer used in this study is 6:1, giving the output torque of the gearbox as 31.5 N·m, with output speed of 666.6 rpm (4000/6). The arrangement of ICE, reducer, linear generator and load is shown in Fig. 8.

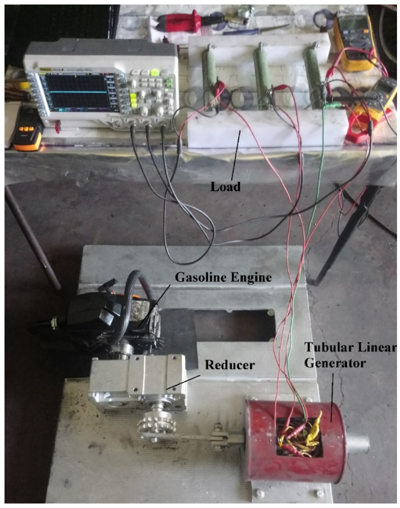

Fig. 8. Linear generator system with ICE drive

Preliminary testing was carried out to eliminate mechanical problems. Different stroke lengths were achieved by placing mount holes in different locations along the length of the crank of the reducer. A laser displacement sensor (Micro-Epsilon ILD 1420 model) was used to measure shaft displacement accurately. The output of the sensor is shown in Fig. 9.

Figure 9 shows the displacement of the shaft and indicates vibration was occurring. After correcting the error, the displacement is seen to have a sinusoidal form. The stroke length is determined from the extremes of displacement, in this instance 102.0965 mm.

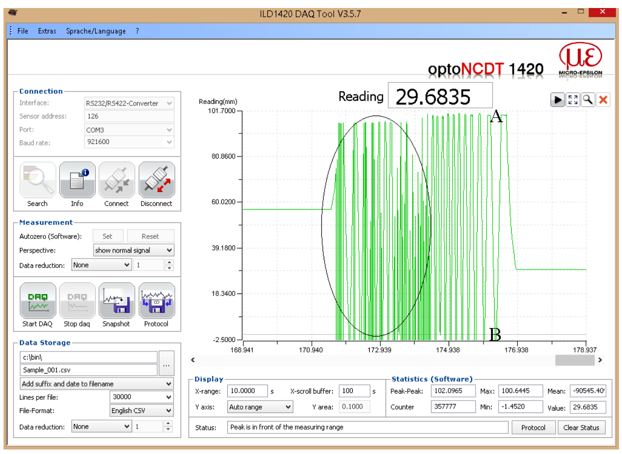

Fig. 9. Displacement of the moving component

Test and experiment results. The speed of the ICE shaft was measured with a laser tachometer and the speed of the linear generator determined from the reducer ratio. The induced voltage of the linear generator versus speed of rotation in the no-load condition is shown in Fig. 10.

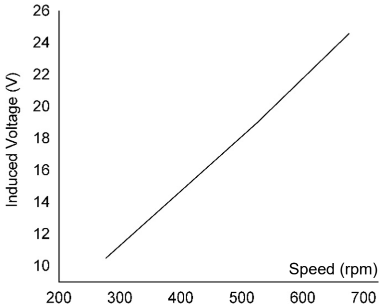

Fig. 10. Induced voltage versus linear generator rotation speed

Figure 10 indicates that the induced voltage increases with rotation speed in the no-load condition, and is 0.0353 V/rpm (2.12 V·s/rad). This would indicate that the results from FEA agree with experiment. The induced voltage at no-load condition for generator rotation speed of 277 rpm (engine speed 1664 rpm) is shown in Fig. 11 and for 525 rpm (engine speed 3150 rpm) in Fig. 12.

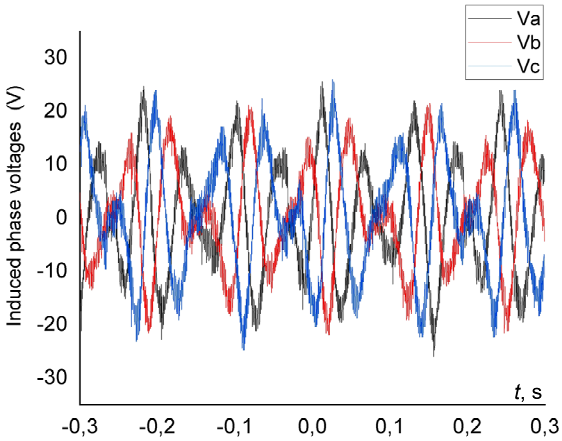

Fig. 11. Phase voltages measured with an oscilloscope at 277 rpm

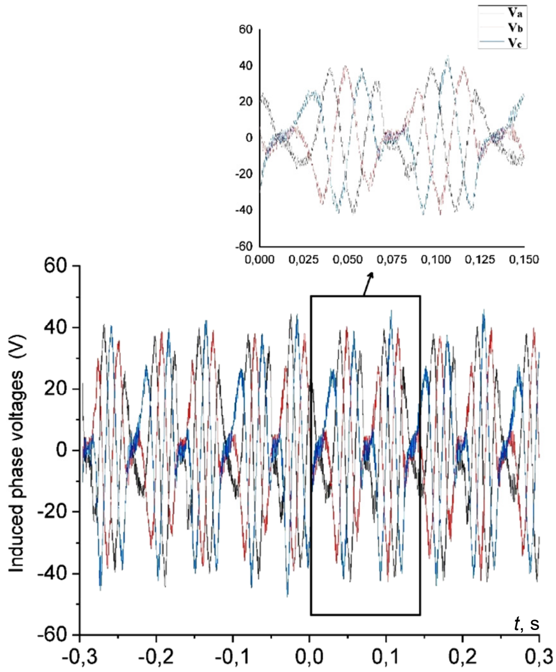

Fig. 12. Phase voltages measured with an oscilloscope at 525 rpm

An expanded version of the induced voltage at generator rotation speed of 528 rpm is given in Fig. 13.

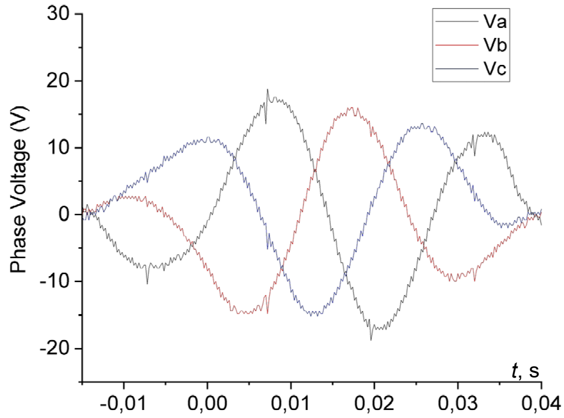

Fig. 13. Phase voltage change according to generator rotation speed of 528 rpm

Figure 13 shows that the phase voltage in each of the three phases. When the shaft is in mid position of travel and magnets pass windings, there will be sinusoidal waveform, but as the shaft approaches extreme of travel, it will slow and reverse direction. This will have the effect of modulating the amplitude of the waveform. At mid travel, the waveform has a higher frequency than at the extremes due to higher speed of the shaft. The waveform inverts when the direction of the shaft changes. The amplitude of V_t (voltage, $V(t)$) in each generator shown in Fig. 13 and Fig. 14 is less than the magnitude of E_f (Fig. 3 and Fig. 10) due to the resistance (R_{phase}) and inductance (L_{phase}) of each winding. Since the linear generator works at a fixed stroke distance, the frequency changes in response to the speed of the engine.

Figure 14 shows how induced voltage increases with generator rotation speed and load resistance. Figure 15 shows how the phase current increases with generator rotation speed and decreases with load resistance.

Conclusions.

1. This study investigates the performance of a linear generator through numerical analysis with finite element analysis and with a practical linear generator driven by an internal combustion engine. Both no-load and loaded conditions were examined by numerical analysis and practical measurement to characterise the linear generator.

2. A tubular type linear generator was produced for test. A reducer was used to connect the crankshaft of the internal combustion engine to the linear generator to match the speed of the engine to the working speed of the linear generator and overcome problems of engine vibration at low engine speed.

3. Stroke length and frequency increase the induced voltage and thus output power. The voltage and power obtained from the linear generator were found to be sufficient for battery charging.

4. If the practical issues of the linear generator, such as bearings and control of the speed of the internal combustion engine can be achieved, then the linear generator can be used in place of the rotating generator. However, as the travel of a piston in the internal combustion engine is limited, the stroke length in the linear generator will likewise be limited. Stroke length can be increased by connecting rod mechanisms.

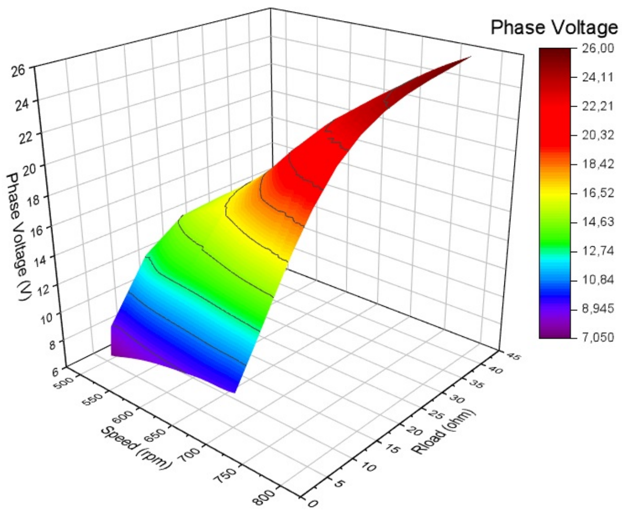

Fig. 14. Phase voltage versus generator rotation speed and load resistance

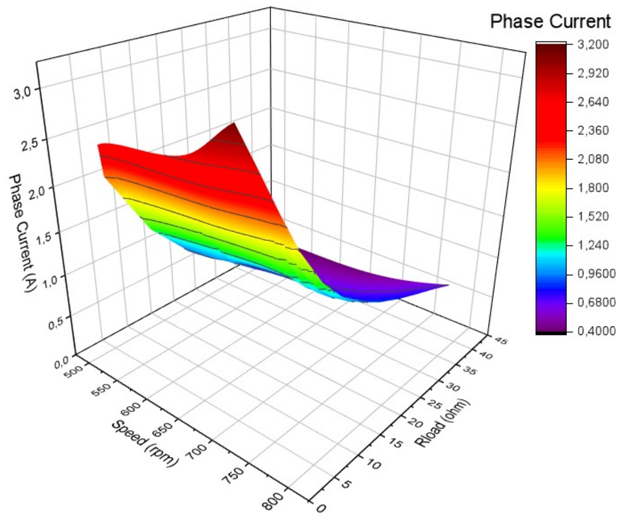

Fig. 15. Phase current versus generator rotation speed and load

Acknowledgements. This work was supported by the Scientific and Technological Research Council of Turkey (TUBITAK 1512) under Grant Number 2180435. Ansys Maxwell software used in this study was provided by Harran University Scientific Research Project Unit (Project No: 18060).

Conflict of interest. The authors declare that they have no conflicts of interest.

REFERENCES

1. Jia B., Smallbone A., Zuo Z., Feng H., Roskilly A.P. Design and simulation of a two- or four-stroke free-piston engine generator for range extender applications. *Energy Conversion and Management*, 2016, vol. 111, pp. 289-298. doi: https://doi.org/10.1016/j.enconman.2015.12.063.

2. Guo C., Feng H., Jia B., Zuo Z., Guo Y., Roskilly T. Research on the operation characteristics of a free-piston linear generator: Numerical model and experimental results. *Energy Conversion and Management*, 2017, vol. 131, pp. 32-43. doi: https://doi.org/10.1016/j.enconman.2016.11.010.

3. Chiang C.-J., Yang J.-L., Lan S.-Y., Shei T.-W., Chiang W.-S., Chen B.-L. Dynamic modeling of a SI/HCCI free-piston engine generator with electric mechanical valves. *Applied Energy*, 2013, vol. 102, pp. 336-346. doi: https://doi.org/10.1016/j.apenergy.2012.07.033.

4. Schneider S., Rinderknecht F., Friedrich H.E. Design of future concepts and variants of The Free Piston Linear Generator. *2014 Ninth International Conference on Ecological Vehicles and Renewable Energies (EVER)*, 2014, pp. 1-8. doi: https://doi.org/10.1109/EVER.2014.6844029.

5. Mao J., Zuo Z., Feng H. Parameters coupling designation of diesel free-piston linear alternator. *Applied Energy*, 2011, vol. 88, no. 12, pp. 4577-4589. doi: https://doi.org/10.1016/j.apenergy.2011.05.051.

6. Miao Y., Zuo Z., Feng H., Guo C., Song Y., Jia B., Guo Y. Research on the Combustion Characteristics of a Free-Piston Gasoline Engine Linear Generator during the Stable Generating Process. *Energies*, 2016, vol. 9, no. 8, art. no. 655. doi: https://doi.org/10.3390/en9080655.

7. Xiao J., Li Q., Huang Z. Motion characteristic of a free piston linear engine. *Applied Energy*, 2010, vol. 87, no. 4, pp. 1288-1294. doi: https://doi.org/10.1016/j.apenergy.2009.07.005.

8. Aichlmayr H.T., Kittelson D.B., Zachariah M.R. Micro-homogeneous charge compression ignition (HCCI) combustion: Investigations employing detailed chemical kinetic modeling and experiments. *Chemical and Physical Processes in Combustion, Fall Technical Meeting, The Eastern States Section*, 2001, pp. 384-387.

9. Mikalsen R. *An investigation into the free-piston engine concept and its potential for high efficiency and low emissions power generation. PhD Thesis*. Newcastle University, United Kingdom, 2008. 192 p. Available at: http://theses.ncl.ac.uk/jspui/handle/10443/3145 (Accessed 16 March 2022).

10. Hong S., Choi H.-Y., Lim J.-W., Lim H.-J., Jung H.-K. Analysis of tubular-type linear generator for free-piston engine. *Renewable Energy and Power Quality Journal*, 2007, vol. 1, no. 05, pp. 719-722. doi: https://doi.org/10.24084/repqj05.365.

11. Hu Y., Xu Z., Sun Y., Liu L. Electromagnetic Characteristics Analysis of a Tubular Moving Magnet Linear Generator System. *Applied Sciences*, 2020, vol. 10, no. 11, art. no. 3713. doi: https://doi.org/10.3390/app10113713.

12. Ahmed T. Raheem, A. Rashid A. Aziz, Saiful A. Zulkifli, Abdalrazak T. Rahem, Wasiu B Ayandotun. Development, Validation, and Performance Evaluation of An Air-Driven Free-Piston Linear Expander Numerical Model. *Evergreen*, 2022, vol. 9, no. 1, pp. 72-85. doi: https://doi.org/10.5109/4774218.

13. Wu L., Feng H., Jia B., Tang Z., Yan X., Wang W. A novel method to investigate the power generation characteristics of linear generator in full frequency operation range applied to opposed-piston free-piston engine generator _ Simulation and test results. *Energy*, 2022, vol. 254, art. no. 124235. doi: https://doi.org/10.1016/j.energy.2022.124235.

14. Hanipah M.R., Mikalsen R., Roskilly A.P. Recent commercial free-piston engine developments for automotive applications. *Applied Thermal Engineering*, 2015, vol. 75, pp. 493-503. doi: https://doi.org/10.1016/j.applthermaleng.2014.09.039.

15. Hung N.B., Lim O. A review of free-piston linear engines. *Applied Energy*, 2016, vol. 178, pp. 78-97. doi: https://doi.org/10.1016/j.apenergy.2016.06.038.

16. Jia B., Zuo Z., Feng H., Tian G., Roskilly A.P. Investigation of the Starting Process of Free-piston Engine Generator by Mechanical Resonance. *Energy Procedia*, 2014, vol. 61, pp. 572-577. doi: https://doi.org/10.1016/j.egypro.2014.11.1173.

17. Zulkifli S.A., Karsiti M.N., Aziz A.R.A. Starting of a free-piston linear engine-generator by mechanical resonance and rectangular current commutation. *2008 IEEE Vehicle Power and Propulsion Conference*, 2008, pp. 1-7. doi: https://doi.org/10.1109/VPPC.2008.4677748.

18. Zulkifli S.A., Karsiti M.N., A-Aziz A.-R. Investigation of linear generator starting modes by mechanical resonance and rectangular current commutation. *2009 IEEE International Electric Machines and Drives Conference*, 2009, pp. 425-433. doi: https://doi.org/10.1109/IEMDC.2009.5075241.

19. Zulkifli S.A., Karsiti M.N., Abd. Rashid Abd. Aziz. Rectangular current commutation and open-loop control for

starting of a free-piston linear engine-generator. *2008 IEEE 2nd International Power and Energy Conference*, 2008, pp. 1086-1091. doi: https://doi.org/10.1109/PECON.2008.4762637.
20. Li Y., Zuo Z., Feng H., Jia B. Parameters matching requirements for diesel free piston linear alternator start-up. *Advances in Mechanical Engineering*, 2015, vol. 7, no. 3, pp. 1-8. doi: https://doi.org/10.1177/1687814015574408.
21. Kim Y.W., Lim J.W., Jung H.K. Starting mode analysis of flat-type linear generator for free-piston engine. *The Transactions of The Korean Institute of Electrical Engineers*, 2008, vol. 57, no. 6, pp. 966-971.
22. Hanipah M.R., Razali A.R. The numerical assessment of motion strategies for integrated linear motor during starting of a free-piston engine generator. *IOP Conference Series: Materials Science and Engineering*, 2017, vol. 257, art. no. 012054. doi: https://doi.org/10.1088/1757-899X/257/1/012054.
23. Song Y., Feng H., Zuo Z., Wang M., Guo C. Comparison Research on Different Injection Control Strategy of CI Free Piston Linear Generator in One-time Starting Process. *Energy Procedia*, 2014, vol. 61, pp. 1597-1601. doi: https://doi.org/10.1016/j.egypro.2014.12.180.
24. Abdulwehab A.I., Ezrann Zharif B. Zainal A., Rashid A.A., Saiful A.Z. Effect of Injection Timing on the Operation of Hydrogen-Fuelled Free-Piston Linear Generator Engine during Starting. *International Journal of Automotive Engineering*, 2013, vol. 4, no. 2, pp. 47-53. doi: https://doi.org/10.20485/jsaeijae.4.2_47.
25. Eid A.M., Suh K. -Y., Choi K. -J., Han H. -D., Lee H. -W., Nakaoka M. A Unique Starting Scheme of Linear-Engine Tubular PM Linear Generator System Using Position Feedback Controlled PWM Inverter. *2006 37th IEEE Power Electronics Specialists Conference*, 2006, pp. 1-5. doi: https://doi.org/10.1109/PESC.2006.1712166.
26. Wang X., Chen F., Zhu R., Yang G., Zhang C. A Review of the Design and Control of Free-Piston Linear Generator. *Energies*, 2018, vol. 11, no. 8, art. no. 2179. doi: https://doi.org/10.3390/en11082179.
27. Arslan S., Gurdal O. Polygonal tubular linear permanent magnet generator analysis and experimental test. *Scientia Iranica*, 2022, vol. 29, no. 1, pp. 168-182. doi: https://doi.org/10.24200/sci.2019.50094.2739.
28. Arslan S., Gurdal O., Akkaya Oy.S. Design and optimization of tubular linear permanent-magnet generator with performance improvement using response surface methodology and multi-objective genetic algorithm. *Scientia Iranica*, 2020, vol. 27, no. 6, pp. 3053-3065. doi: https://doi.org/10.24200/sci.2018.50093.1506.
29. Virsik R., Heron A. Free piston linear generator in comparison to other range-extender technologies. *2013 World Electric Vehicle Symposium and Exhibition (EVS27)*, 2013, pp. 1-7. doi: https://doi.org/10.1109/EVS.2013.6914925.
30. Serdal A., Gurdal O. Hibrit Araçlar İçin Serbest Pistonlu Doğrusal Jeneratör Çeşitlerinin İncelenmesi. *Mesleki Bilimler Dergisi*, 2017, vol. 6, no. 3, pp. 540-552. (Tur).
31. Cheng C.-H., Dhanasekaran S. Numerical Analysis and Parametric Study of a 7 kW Tubular Permanent Magnet Linear Alternator. *Sustainability*, 2021, vol. 13, no. 13, art. no. 7192. doi: https://doi.org/10.3390/su13137192.
32. Rymsha V.V., Radimov I.N., Gulyy M.V., Merkulov I.V. Motorsolve software package: verification of parameters and characteristics of the brushless permanent magnet motor. *Electrical Engineering & Electromechanics*, 2019, no. 5, pp. 20-24. doi: https://doi.org/10.20998/2074-272X.2019.5.03.
33. Bianchi N., Bolognani S., Cappello A.D.F. Back EMF improvement and force ripple reduction in PM linear motor drives. *2004 IEEE 35th Annual Power Electronics Specialists Conference (IEEE Cat. No.04CH37551)*, 2004, vol. 5, pp. 3372-3377. doi: https://doi.org/10.1109/PESC.2004.1355071.
34. Panchal T.H., Patel A.N., Patel R.M. Reduction of cogging torque of radial flux permanent magnet brushless DC motor by magnet shifting technique. *Electrical Engineering & Electromechanics*, 2022, no. 3, pp. 15-20. doi: https://doi.org/10.20998/2074-272X.2022.3.03.
35. Tajdiny A., Monsef H., Lessani H. Design and analysis of a novel yokeless mover permanent magnet linear generator for free piston engine converter. *IET Electric Power Applications*, 2021, vol. 15, no. 10, pp. 1314-1330. doi: https://doi.org/10.1049/elp2.12101.

Received 03.06.2022
Accepted 11.09.2022
Published 06.01.2023

Serdal Arslan[1]*, Assistance Professor,*
Hacene Mellah[2]*, PhD,*
[1] Department of Electrical,
Harran University Organized Industrial Zone Vocational High School,
Harran University, Sanliurfa, Turkey,
e-mail: serdalarslan@harran.edu.tr (Corresponding Author)
[2] Department of Electrical Engineering,
Akhli Mohend Oulhadj University, Bouira, Algeria,
e-mail: has.mel@gmail.com

How to cite this article:
Arslan S., Mellah H. Analysis and testing of internal combustion engine driven linear alternator. *Electrical Engineering & Electromechanics*, 2023, no. 1, pp. 3-9. doi: https://doi.org/10.20998/2074-272X.2023.1.01